Improvement of a functional method to determine the design thermal transmittance of building façades. Implementation in southern Spain

J.M. Pérez-Bella, J. Domínguez-Hernández, E. Cano-Suñén, M. Alonso-Martínez, J.J. del Coz-Díaz

PII: S2352-7102(19)32560-4

DOI: https://doi.org/10.1016/j.jobe.2020.101231

Reference: JOBE 101231

To appear in: *Journal of Building Engineering*

Received Date: 18 November 2019

Revised Date: 28 January 2020

Accepted Date: 29 January 2020

Please cite this article as: J.M. Pérez-Bella, J. Domínguez-Hernández, E. Cano-Suñén, M. Alonso-Martínez, J.J. del Coz-Díaz, Improvement of a functional method to determine the design thermal transmittance of building façades. Implementation in southern Spain, *Journal of Building Engineering* (2020), doi: https://doi.org/10.1016/j.jobe.2020.101231.

Improvement of a functional method to determine the design thermal transmittance of building façades. Implementation in southern Spain

J.M. Pérez-Bella[a] (ORCID 0000-0003-4278-6622) jmpb@unizar.es

J. Domínguez-Hernández[a,*] (ORCID 0000-0002-3776-9791) javdom@unizar.es

E. Cano-Suñén[a] (ORCID 0000-0001-5137-2478) ecs@unizar.es

M. Alonso-Martínez[b] (ORCID 0000-0003-2968-3960) mar@constru.uniovi.es

J.J. del Coz-Díaz[b] (ORCID 0000-0001-6101-1537) juanjo@constru.uniovi.es

[a] *Department of Construction Engineering, Engineering and Architecture School, University of Zaragoza, María de Luna s/n, 50018, Zaragoza, Spain.*

[b] *Department of Construction Engineering, University of Oviedo, Edificio Departamental Viesques nº 7, 33204 Gijón, Spain.*

* **Corresponding author:** Dr. Javier Domínguez-Hernández.

Department of Construction Engineering, University of Zaragoza,

Campus Río Ebro, Edificio Betancourt, María de Luna s/n, 50018, Zaragoza, Spain.

Tel.Fax: +34 976 76 21 00. E-mail: javdom@unizar.es

Improvement of a functional method to determine the design thermal transmittance of building façades. Implementation in southern Spain

Abstract

The thermo-hygrometric conditions to which construction materials are subjected cause their thermal performance to vary by location. These variations must be characterised in order to design building envelopes adjusted to the requirements of each situation, thus contributing to improve their energy efficiency under actual operating conditions. To this end, a functional calculation procedure that corrects the standardised thermal conductivity values of façade materials (λ-value) has been recently proposed; which considers the climatic characteristics of each location. This work proposes and validates improvements that, while preserving its functionality, overcome some limitations of the original procedure. To calculate more accurate corrections, the façade configuration and the climatic zones established by the building codes are also considered, allowing a more reliable characterisation of the design thermal transmittance of each building façade. By using climatic records gathered from 316 weather stations, a detailed isopleth map is also developed to present the applicable corrections for more than 250,000 km^2 of southern Spain. The largest λ-value corrections are identified on the southeast coast and reach up to +6% in the summer months (with average annual corrections above +4%). This improved procedure can be extrapolated to any national building code that establishes constant values of thermal conductivity for façade materials and that defines thermal design requirements based on climatic zones.

Keywords

Thermal conductivity; Façade materials; Climatic data; Building codes; Spain

1. Introduction

The usually porous nature of construction materials causes a variable amount of moisture and liquid water to be stored inside, increasing their thermal conductivity regarding the dry state [1-3]. Likewise, the heating of the material (and of the molecules of liquid and gas present inside) also increases the transport of energy and reduces the thermal insulation of the material [4-6].

The construction materials used in building enclosures are particularly exposed to atmospheric conditions that modify their moisture content and temperature (e.g., solar radiation, precipitation and wind). Sometimes these conditions are transitory, such as the action of wind-driven rain. In other cases, its effect depends on the orientation, latitude, height, surroundings or construction quality of each building [7-9]. As a result, the heat transfer through the building envelope constitutes a complex and dynamic phenomenon, the detailed characterisation of which requires exhaustive simulations for each possible configuration of the constructive element and environmental condition [10-13].

Despite this, most construction standards establish constant hygrothermal properties for building materials that are applicable to any location and situation [14-17]. To define these properties, standardised conditions of temperature and moisture content are considered, which usually coincide with those established for the declared thermal values provided by the manufacturers of construction materials [18].

Among these properties, the thermal conductivity or λ-value is repeatedly used by building codes to establish the thermal requirements of buildings, setting the maximum thermal transmittance (U-value) of the enclosures [19-21]. Thus, although considering constant λ-values simplifies the building thermal design, it also introduces an underlying error in the subsequent calculation or simulation [22-26]. In professional practice, the use of resources to adjust the thermal conductivity according to the environmental conditions (e.g., standard ISO 10456 or specialised software) is usually ruled out given the greater calculation effort, its economic cost or the lack of the required input data [18, 27].

As an alternative, a procedure has recently been developed that without significantly increasing the calculation effort provides design λ-values for façade materials adapted to the climatic conditions of each location [28]. This novel procedure renounces a dynamic characterisation of the heat transfer through the enclosure, considering only average, maximum or minimum situations of the thermo-hygrometric conditions that permanently

act on the building façade (temperature and relative humidity, both inside and outside the building). Multiplying the constant λ-values provided by the construction standards by a correction factor based on these representative climatic conditions, this procedure obtains more realistic λ-values and so an accurate design U-value of the façade at each location.

Until now, the development of this procedure has focused on traditional façade systems with a significant proportion of masonry elements. So far, the correction factors have been characterised considering the climatic conditions in 52 provincial capitals of Spain and exhaustively in the territory of two regions in Northeast Spain (Aragon and Catalonia) [28-29]. The validations performed in these studies, by analysing façades with one or two masonry layers and interior insulation, confirm the utility of the procedure. This correction allows practitioners to adjust, in a simple and functional way, the standardised λ-values, obtaining results similar to those that could be calculated through standard ISO 10456.

This article takes a step forward by using this procedure to exhaustively identify the correction factors applicable in more than 250,000 km^2 of southern Spain. A new detailed isopleth map will also facilitate this correction of the standardised λ-values, even in locations without representative climatic data. In turn, the weaknesses of the methodology will be analysed, proposing improvements related to its applicability to different façade configurations and its better adaptation to the design requirements established by building codes in each climatic zone. The Spanish Building Technical Code (SBTC) will be taken as an example [21]. Finally, these improvements will be validated in three large urban areas (Madrid, Valencia and Seville) and for different façade configurations.

Overall, this work minimises the intrinsic limitations of this novel calculation procedure by improving its applicability and accuracy in any situation. In particular, it allows refining the λ-values currently used by thermal designs based on the SBTC for a vast region of Spain. Known the influence of the envelope U-values on the building energy use, the aim of this research is to progress in functional envelope designs that consider the actual hygrothermal properties of construction materials under their operating conditions [30-32].

2. Background

Variations in temperature and moisture content have different effects on the thermal conductivity of each material. Therefore, to assess in detail the hygrothermal behaviour of a façade, it is necessary to identify the properties of all the materials incorporated in its design (e.g., their moisture sorption isotherms) [5, 10, 13, 23, 25, 30-34]. In addition, the environmental conditions on each material must be determined, which depend on its position in the façade and the internal and external operating conditions [10, 13, 35]. These conditions also change when the thickness, position and nature of any of the layers are modified. The result is an iterative, laborious and non-functional calculation process, given the multiple possibilities that thermal and construction design entail [36].

Hence, although the building codes recommend using design λ-values (i.e., conductivity values adapted to the actual conditions of the material in its intended location and construction configuration), there are also established alternatives that reduce the calculation complexity. One of the most frequent is to suppose a common environmental condition for all materials [19-21, 37-38]. This environmental design condition usually agrees with that used to determine the λ-values collected in the construction standards and, in turn, with one of the reference conditions established for the declared λ-values provided by the manufacturers of construction materials (see Table 1). Thus, in practice, all these standardised λ-values can be incorporated without distinction into the thermal calculation without further conversions.

As a result, although different thermal requirements are defined according to the climatic zone, usually the building thermal design do not consider the different behaviour of materials at each location and façade configuration due to the environmental conditions that they support.

Table 1. The four reference conditions (Ia, Ib, IIa, and IIb) established by standard ISO 10456 for declared thermal values.

To reverse this situation, a procedure has recently been developed that, without increasing the calculation effort, allows adjusting the standardised λ-values of façade materials considering the environmental conditions of each location [28]. To this end, the formulation collected in standard ISO 10456 (Eq. 1) was taken as the starting point, which defines a temperature conversion factor F_T (-) and a moisture conversion factor F_M (-) to relate the λ-value (W/m·K) of a material under two different environmental conditions (1 and 2). The environmental condition

used by the construction standards (i.e., one of those set for the declared λ-values) would be adopted as condition 1, while the actual environmental condition of the material under its operating conditions would correspond to condition 2 [18]. Since the standardised value usually incorporates the ageing effect, an ageing conversion factor is not considered.

$$\lambda_2 = \lambda_1 \cdot F_T \cdot F_M \tag{1}$$

The calculation of each conversion factor depends on the difference of temperature T (°C) and moisture content ψ (m^3/m^3) of the material between both environmental conditions and the intrinsic conversion coefficients f_T (K^{-1}) and f_ψ (m^3/m^3) compiled in standard ISO 10456 for different materials (Eq. 2).

$$\lambda_2 = \lambda_1 \cdot e^{f_t(T_2-T_1)} \cdot e^{f_\psi(\psi_2-\psi_1)} \tag{2}$$

To avoid the need to determine the temperature and moisture content in each layer of the wall (as in standard ISO 10456), this new procedure considers a single material in the façade. The homogeneous properties of this uniform material would be representative of those of the insulation and masonry products commonly used in traditional façade systems [28]. Considering that the thermal insulating materials compiled in the standard ISO present an average value of f_T equal to 0.00475 K^{-1} and equal to 0.002 K^{-1} for masonry materials, both values were combined to obtain a simplified conversion coefficient $f_{T\,uniform}$ (K^{-1}) for this hypothetical uniform material. To this end, a weighting based on the percentage contribution ($R_{contribution}$) of both families of materials (i.e., insulations and masonry products) to the thermal resistance of the enclosure is established [28]. Starting from the average value of f_ψ coefficients tabulated for insulating materials (3.4 m^3/m^3) and for masonry materials (7.0 m^3/m^3) in ISO 10456, it is possible to use the same weighting to obtain a simplified conversion coefficient $f_{\psi\,uniform}$ (m^3/m^3) for the uniform material (Eqs. 3 and 4).

$$f_{t\,uniform} = f_{t\,insulation} \cdot R_{contribution} + f_{t\,masonry} \cdot \left(1 - R_{contribution}\right) \tag{3}$$

$$f_{\psi\,uniform} = f_{\psi\,insulation} \cdot R_{contribution} + f_{\psi\,masonry} \cdot \left(1 - R_{contribution}\right) \tag{4}$$

Analysing only 25 traditional façade configurations, an average contribution of thermal insulating materials to the thermal resistance of the façades of 56.5% (i.e., 43.5% from masonry materials) was proposed [28-29].

Adopting a $R_{contribution}$ value equal to 0.565, fixed values were determined for the simplified coefficients $f_{T\ uniform}$ and $f_{\psi\ uniform}$: 0.0036 K^{-1} and 4.96 m^3/m^3, respectively.

Assuming that the façade consists of a single layer of uniform material, its average temperature under operating conditions (T_2) can be determined as the simple average between the outdoor temperature (T_{ext}) and indoor temperature (T_{int}) (Eq. 5).

$$T_2 = \frac{T_{ext} + T_{\text{int}}}{2} \tag{5}$$

Conversely, determining the water content present in the uniform material requires a more elaborate approach because each construction material is characterised by a moisture sorption isotherm that relates its moisture content ψ to the environmental relative humidity RH [1-3, 33-34, 39]. Thus, this new procedure proposed a generalised sorption isotherm intended to be representative of the isotherms of materials commonly used in traditional façade systems. For simplicity, a linear isotherm that relates the moisture content in the dry state (RH 0% and 0 m^3/m^3) and the moisture content that the material would present at a RH of 80% (ψ_{80} m^3/m^3) was used [28].

Some databases collect the values of ψ_{80} for usual façade materials, allowing estimations of average ψ_{80} values for thermal insulating materials (0.0052 m^3/m^3) and for masonry materials (0.0129 m^3/m^3) [27-28]. Considering again the weighting established by the $R_{contribution}$ value, Eq. 6 was used to determine a representative $\psi_{80\ uniform}$ value for his hypothetical material.

$$\psi_{80\ uniform} = \psi_{80\ insulation} \cdot R_{contribution} + \psi_{80\ masonry} \cdot \left(1 - R_{contribution}\right) \tag{6}$$

The linear sorption isotherm that relates the moisture content of this uniform material is defined by Eq. 7 (the same $R_{contribution}$ = 0.565 value indicated before can be applied).

$$\psi_{RH\ uniform} = RH_{uniform} \cdot \frac{0.0052 \cdot R_{contribution} + 0.0129 \cdot \left(1 - R_{contribution}\right)}{0.8} \tag{7}$$

$RH_{uniform}$ (-) represents the relative humidity in the uniform material, which can be obtained from psychometric formulae (Eq. 8) that relate the vapour pressure P_v (Pa) in the indoor and outdoor environmental conditions (*int* and *ext*, respectively) and the saturation vapour pressure P_{sat} (Pa) for T_2 (temperature of the uniform material) [40].

$$RH_{uniform} = \frac{\left(P_{v\,ext} + P_{v\,int}\right)/2}{P_{sat\ T_2}} = \frac{\left(P_{v\,ext} + P_{v\,int}\right)/2}{610.5 \cdot e^{\frac{17.269 \cdot T_2}{237.3 + T_2}}} \tag{8}$$

Substituting the factors developed above into Eq. 2, generalised equations were obtained to correct the standardised λ-value of façade materials (Eqs. 9-11). A new conductivity correction factor *CCF* (-) was thus defined that is applicable to the λ-values established by construction standards and building codes (λ_1) and allows approximating a design λ-value adjusted to the real operating conditions at each location (λ_2) [28].

$$\lambda_2 \approx \lambda_1 \cdot CCF = \lambda_1 \cdot F_T \cdot F_M \tag{9}$$

$$F_T = e^{\left[0.00475 \cdot R_{contribution} + 0.002 \cdot \left(1 - R_{contribution}\right)\right] \cdot \left[\left(\frac{T_{ext} + T_{int}}{2}\right) - T_1\right]} \tag{10}$$

$$F_M = e^{\left[3.4 \cdot R_{contribution} + 7 \cdot \left(1 - R_{contribution}\right)\right] \cdot \left[\left(\frac{\left(P_{v\,ext} + P_{v\,int}\right)/2}{610.5 \cdot e^{\frac{17.269 \cdot \left(\frac{T_{ext} + T_{int}}{2}\right)}{237.3 + \left(\frac{T_{ext} + T_{int}}{2}\right)}}} - RH_1\right) \cdot \left(\frac{0.0052 \cdot R_{contribution} + 0.0129 \cdot \left(1 - R_{contribution}\right)}{0.8}\right)\right]} \tag{11}$$

Applying the $R_{contribution}$ value (0.565) and the environmental conditions established as a reference for construction materials by each building code (T_1 and RH_1), this general formulation is simplified. The CCF value depends only on the indoor and outdoor environmental conditions considered for the façade. Thus, the necessary correction at each location can be obtained from the T and P_v values inside the building (established to guarantee the comfort of the occupants) and from external climatic conditions representative at the location (e.g., annual average values of T and RH).

Focusing on the Spanish case, the SBTC establishes 10°C and an equilibrium moisture content at 23°C and 50% RH (i.e., the Ib reference condition established by ISO 10456) as environmental condition to define the standardised λ-value of construction materials (λ_{Ib}-values). By also adopting the interior comfort conditions established for dwellings and places without high humidity production (20°C and RH of 55%), Eqs. 9-11 can be simplified until obtaining Eq. 12 [18, 21, 40]. The coefficients of this equation may vary by country, depending on

the environmental conditions established for the standardised λ-values, the considered interior conditions and the applied $R_{contribution}$ value.

$$\lambda_{design\ Spanish\ façades} \approx \lambda_{Ib\ (SBTC)} \cdot e^{0.0036 \cdot \left(\frac{T_{ext}+20}{2}-10\right)} \cdot e^{0.0531 \cdot \left(\frac{\left(RH_{ext} \cdot P_{sat\ ext}+1285.3\right)/2}{610.5 \cdot e^{\left(\frac{17.269 \cdot \left(\frac{T_{ext}+20}{2}\right)}{237.3+\left(\frac{T_{ext}+20}{2}\right)}\right)}} - 0.55 \right)} \quad (12)$$

The application of Eq. 12 in previous works has allowed the identification of the CCF values applicable in 52 Spanish cities (provincial capitals) as well as exhaustively in northeastern Spain [28-29]. These studies have shown the need to consider design λ-values for façade materials higher than those currently fixed by the SBTC, mainly due to the difference between the reference 10°C and the usual high temperatures in the country.

Although the functional advantages of this correction factor are clear, the calculation procedure also features certain weaknesses: the correction accuracy decreases the more the façade differs from the archetype model adopted by the method (i.e., $R_{contribution}$ value equal to 0.565 and traditional façade systems). Therefore, the CCF values can offer limited improvements for certain types of façades (e.g., lightweight façades, external wall insolation systems or walls with a greater proportion of insulating material, in line with the requirements for nearly zero-energy buildings) [41]. The procedure also does not consider the predominance of certain façade configurations in each climatic zone as a result of the maximum U-values required by the building codes. In turn, the analysis of the Spanish territory remains incomplete (only some northeastern zones and several isolated cities have been characterised). Among the unexamined regions, southern Spain stand out because the high ambient temperatures, making foreseeable a greater need for correcting the standardised λ_{Ib}-values.

Next, the scope of these previous studies is broadened, incorporating the exhaustive characterisation of the south of Spain (almost 50% of the surface of the country), by the analysis of climatic records obtained in 316 weather stations (Fig. 1). The CCF values identified at each point (considering average annual records of T and RH) allow a detailed isopleth map for the entire territory to be produced. In addition, calculation improvements that allow adjusting the original CCF values according to the type of façade and the design requirements imposed by building codes in climatic zones are proposed. Finally, the effectiveness of these improvements is verified by studying

different façade configurations subjected to diverse environmental conditions of this Spanish area. Although this calculation improvement is presented by using climatic zones and façade configurations valid in Spain, analogous results for other countries could be obtained by the same methodology.

Figure 1. Extension of the application scope and improvements proposed for the calculation procedure.

3. Characterisation of the corrections in southern Spain

In this section, the procedure described above is used to identify the corrections for standardised λ_{lb}-values of façade materials in 316 Spanish locations. The study analyses monthly climatic records of temperature and relative humidity that were collected during periods of up to 16 years (in most cases 10 to 15 years of records are available) at weather stations distributed throughout the regions of Andalusia, Castile-La Mancha, Community of Madrid, Extremadura, Region of Murcia and Valencian Community (Fig. 2). Stations with less than five years of records were excluded due to their low representativeness, as were those with annual data series with discontinuities.

Figure 2. Territorial distribution of the Spanish weather stations analysed throughout this research. *Darker colours represent higher altitudes*.

The assessed territory is located between latitudes 36°N and 41°N, encompassing the territory of the country characterised by hot-summer Mediterranean climates and semi-arid climates (Csa, BSk and BSh according to the Köppen-Geiger climate classification) [42-43]. These regions present high average temperatures in summer (e.g., Madrid 24.4°C in July; Seville 26.8°C and Valencia 24.5°C in August) and mild winters near the coast (e.g., Seville 10.7°C and Valencia 10.4°C in January). Towards the interior of the Iberian Peninsula, a vast plateau with heights between 600 and 760 m that is rimmed by mountain ranges reaching up to-3,478 m (Mulhacén mountain, in the Baetic System) favours lower average temperatures in winter (e.g., Madrid 6.2°C in January). The relative humidity also shows seasonal oscillations, with higher average annual values in the littoral (Madrid 56.4%, Seville 65.4% and Valencia 64.8%) [40, 43].

Considering that the SBTC establishes an interior comfort temperature equal to 20°C (with an RH of 55%), it can be deduced that during most of the year the façade materials are subject to temperatures and relative humidities greater than those considered for the standardised λ_{Ib}-values (i.e., reference condition Ib). These climatic conditions make correcting these λ_{Ib}-values especially relevant for improving the thermal designs of façades in the analysed zone.

To characterise these regions, meteorological records from different databases have been combined, thus increasing the number of points analysed to reduce the distance between them and minimise the correction uncertainty in intermediate areas [44-48]. The highest concentrations of stations are located on the Mediterranean coast and along the Baetic Depression due to the higher population densities. Extremadura and Castile–La Mancha present smaller and dispersed urban areas, resulting in a less dense arrangement of weather stations. The Community of Madrid, the population of which is concentrated in the capital and its surroundings, is represented by a limited number of stations.

The obtained distribution (1 result per 794 km^2 on average) enables the production of a detailed isopleth map by interpolation, thus allowing the CCF value at any point of the territory to be extrapolated with reasonable accuracy (Table 2). In addition to the 316 stations analysed, records of 25 other peripheral locations have been considered in order to improve the correction isopleths in the perimeter areas of this territory.

Table 2. Distribution of weather stations throughout the 6 analysed regions (25 stations were also analysed in neighbouring regions).

By determining the mean annual temperature and relative humidity at each point (T_{ext}, RH_{ext} and $P_{sat\ ext}$), it is possible to solve Eq. 12 for each location. Therefore, the mean annual CCF values needed to correct the standardised λ_{Ib}-values are obtained. Likewise, it would be possible to identify the monthly CCF values (considering the mean temperature and mean relative humidity of each month) or the correction values applicable in other countries and climatic conditions.

These calculated CCF values are compiled in Table 3 (consult the linked Research data for an extended table), in which the months of extreme corrections are also indicated. The CCF values (mean, maximum and minimum) are presented as percentages (i.e., the λ_{Ib}-value percentage increase), thus reducing the number of decimal places required (e.g., a CCF value of 1.0416 is equivalent to a percentage increase of + 4.16%).

Table 3. Mean annual CCF values identified in southern Spain (maximum and minimum monthly values are also shown). *For succinctness, only the most extreme values are presented.*

As can be seen, the largest corrections are identified in the southeast of Spain (especially in Region of Murcia), with mean annual CCF values that reach up to +4.16% in San Javier. The maximum monthly value is reached in the Valencian Community (Sueca, +6.03% in August). All the analysed stations present the maximum corrections during the summer months, confirming the unfortunate choice of 10°C for the standardised λ-values in Spain (reference condition Ib). In the south coast of the country, the high corrections remain throughout the year, with minimum monthly CCF values that reach up to 2.90% (e.g., Vejer de la Frontera, Sanlucar de Barrameda, and Vélez-Málaga).

The lowest mean annual CCF values are identified in Prados Redondos, Cañete and Mariana, all of which are located near the Iberian System (+2.43%, +2.59% and +2.60%, respectively). In addition, Prados Redondos and Cañete present the minimum monthly values (+1.42% and +1.49%, both in January). These corrections are consistent with colder environmental conditions throughout the year, which are caused for the altitude of these mountain areas.

It can be emphasised that all the stations show a need to increase the λ_{Ib}-value (even during the winter months). This confirms the poor general reliability of the λ_{Ib}-values currently used by the SBTC in southern Spain; even under favourable conditions, the thermal design ascribes an insulating performance to façade materials that exceed the actual value. Although the choice of another reference condition would be more reasonable (e.g., the IIb condition, with 23°C as the reference temperature), this solution would still not consider the variation of climatic conditions by location, which is a necessary aspect to progress towards performance-based designs.

By compiling these CCF values an isopleth map has been produced (Fig. 3): A linear interpolation was undertaken to identify the correction at any point in the territory through smoothed isopleths. This interpolation allows an exhaustive characterisation of the entire coast and interior of Andalusia, accepting greater uncertainty towards the interior of the country (given the greater dispersion of weather stations). This map aims to facilitate the implementation of the correction, thus enabling the improvement of the thermal design even in locations without direct meteorological records. Along with the results corresponding to the northeast of Spain (obtained by previous studies), this map completes an exhaustive characterisation of the Spanish Levante and of the central and southern area of the country [29].

Figure 3. Isopleth map of the mean annual CCF (% values) applicable for façade materials in southern Spain.

The greater density of isopleths in the east and southeast of the Iberian Peninsula is explained by the greater number of available stations and by the marked variation in CCF values caused by the proximity of the mountain ranges to the coast. In fact, other areas with high numbers of stations (e.g., the Baetic Depression) show much lower concentrations of isopleths, suggesting more uniform environmental conditions. The presence of Sierra Morena and the Baetic System around this depression is reflected in the map, with minor correction values as the altitude increases. In the Community of Madrid and the eastern part of Castile–La Mancha, the Spanish southern sub-plateau maintains uniform environmental conditions, with stable correction factors until nearing its perimeter mountain ranges. In turn, Extremadura and western Castile–La Mancha present greater variations given the topographic irregularity of the terrain. All this variability justifies the need to develop tools such as those applied in this work to determine the properties of construction materials under their operating conditions, advancing towards performance-based façade designs.

4. Improvements in the calculation procedure considering the façade configuration and climatic zone

Assuming the validity of the conversion coefficients f_T and f_ψ tabulated in the standard ISO 10456, the $R_{contribution}$ value constitutes the main uncertainty parameter for the correction procedure presented previously. Thus,

large variations may occur in the contribution of thermal insulating materials to the thermal resistance of a wall, depending on the façade system and the climatic zone in which it is used. A thorough analysis of this parameter could lead to changes from the original value (i.e., 0.565) and to a substantial improvement in the correction. Next, a procedure improvement for the Spanish case is proposed, which can be adapted to other national building codes following an analogous methodology.

To this end, a computer Catalogue of Constructive Elements (CCE) that complements the SBTC is used; its previous printed version can be consulted to identify up to 273 possible façade configurations used in Spain, which are grouped into 15 specific subgroups according to the general typology of the façade system [17, 49]. For each configuration, the usual thicknesses of the construction elements (except thermal insulation) and its resulting U-values are provided. Thus, the thermal resistance of each façade configuration is defined by the sum of a fixed value (corresponding to the non-insulation materials) and a variable value (corresponding to the thickness and nature of the insulation materials, according to the requirements established for each climatic zone).

The establishment of climatic zoning is a growing topic concerning the energy efficiency and energy consumption of buildings and has been adopted by many national building codes [21, 50-52]. These building codes provide guideline U-values for each climatic zone, which are used for the thermal design of the building envelopes. In this way, the guideline U-values allow to calculate the required thermal insulation for the façade configurations compiled in any catalogue (such as the CCE).

The SBTC defines climatic zoning based on winter and summer climate severity. Climatic zones for winter are identified by a letter (α, A, B, C, D and E, ordered from lowest to highest severity). Climatic zones A, B and C predominate in the regions analysed in this work. Only the southern sub-plateau is identified as zone D, whereas zone E applies only to mountain zones of the Baetic, Central and Iberian systems. Climatic zones for summer are identified by a number: 1, 2, 3 and 4, from lowest to highest severity [21]. Guideline U-values are established for each winter climatic zone, which can be used for calculating a specific $R_{contribution}$ value for each façade configuration included in the CCE (Eq. 13).

$$R_{contribution} = \frac{guideline\ U\text{-}value_{according\ climate\ zone}}{U\text{-}value_{insulating\ material}} = 1 - \frac{guideline\ U\text{-}value_{according\ climate\ zone}}{U\text{-}value_{of\ non\text{-}insulating\ materials\ in\ the\ configuration}} \quad (13)$$

By averaging the calculated $R_{contribution}$ values for the configurations included in each subgroup of façades, it is possible to develop Table 4, where the applicable average values are shown according to these 15 façade subgroups and the intended climatic zone.

Table 4. Mean $R_{contribution}$ values required for each subgroup of façade systems according to the thermal transmittance guideline established by the SBTC for each climatic zone.

As might be expected, the contribution of insulating materials to the thermal resistance of each façade configuration increases with increasing climatic severity. Except in climatic zone α (applicable only in the Canary Islands), $R_{contribution}$ values higher than the value 0.565 initially proposed are obtained in general. The tightening of the U-values required and the limited selection of façades considered to propose the original $R_{contribution}$ value can explain this disparity. In turn, the façade subgroups with less insulating materials present lower $R_{contribution}$ values (e.g., CCE subgroup No. 9, see Table 4).

To increase the correction accuracy, these specific $R_{contribution}$ values can be incorporated into the general formulation (Eqs. 9-11). For practicality, an adjustment for the CCF values based on the $R_{contribution}$ equal to 0.565 has been included. By operating with these equations, this adjustment can be expressed by an exponential value C_A (-) that is dependent on the specific $R_{contribution}$ value applicable to each façade configuration and climatic zone (Eq. 14). In this equation, $CCF_{original}$ represents the absolute value of the correction factor identified through the original procedure and represented in the isopleth map (e.g., 1.0416 for the mean value of San Javier station, review Table 3).

$$\lambda_{design\ Spanish\ facades} \approx \lambda_{Ib\ (STBC)} \cdot \left(CCF_{original} \right)^{C_A} \tag{14}$$

Although these C_A values have been solved for each of the 273 CCE façade configurations, for succinctness, Table 5 shows only the average C_A values of each façade subgroup. In general, the C_A adjustment reduces the original correction in most façade systems and climatic zones (without shading in the table) and is more pronounced for greater climatic severity and contribution of the insulating material to the façade thermal resistance.

Table 5. Proposed factor C_A to adjust the original CCF values identified in Spain, considering façade configuration and climatic zone.

4.1 Validation of procedure improvements

Below, the validity of the exponential values C_A (and of the improved correction procedure) is analysed for different façade configurations located in the three largest urban areas assessed in this work (Madrid, Valencia and Seville). For this validation, the environmental conditions registered at weather stations close to the three cities (St. Fernando de Henares, Moncada and La Rinconada) are adopted. These conditions and other relevant data are compiled in Fig. 4

Figure 4. Annual variation of the monthly $CCF_{original}$ values identified in the largest cities analysed (Madrid, Valencia and Seville) and their mean annual values of temperature and relative humidity.

Fig. 5 shows the 3 analysed façade configurations (representative of different façade subgroups), as well as the properties of their materials (vapour diffusion resistance factor; f_T and f_ψ values) and standardised λ_{lb}-values. For each facade, the specific masonry elements of each configuration defined in the CCE (layers, materials and thicknesses) have been used [42].

Figure 5. Façade configurations and material properties considered for the validation.

In turn, three usual thermal insulation materials are used, considering the thickness necessary to reach the guideline U-value established by the SBTC for the climatic zone of each city (i.e., Madrid 0.27 W/m^2 K; Valencia and Seville 0.38 W/m^2 K). For this, the usual calculation based on the SBTC has been conducted, considering the

standardised λ_{lb}-values, a surface thermal resistance equal to 0.04 m^2K/W for the outside air film and equal to 0.13 m^2K/W for the inside air film (Eq. 15, omitting the conductivity correction factor) [18].

$$U\text{-}value_{design} = \frac{1}{0.04} + \sum_{i=1}^{\#layers} \frac{\lambda_{lb\ i} \cdot \left(CCF_{original}\right)^{C_A}}{Thickness_i} + \frac{1}{0.13} \tag{15}$$

Then, the U-values of these façades have also been calculated by adjusting the standardised λ_{lb}-values using the ISO 10456, considering the conversion factors of each material layer (i) and its specific temperature and relative humidity under the average annual conditions of each city (Fig. 4-5 and Eq. 2). The moisture content of each material layer was obtained from the sorption isotherms collected in the database of the WUFI Light 5.3 software [18, 27].

Finally, the calculation of the U-value is repeated by correcting the standardised λ_{lb}-values by the mean annual $CCF_{original}$ applicable in each city as well as by the mean annual $CCF_{original}$ adjusted by the C_A value (Eq. 15). As can be observed, the correction only need to multiply the current λ_{lb}-values by the CCF value associated with the location and the C_A value corresponding to the façade configuration and climatic zone.

Adopting as a reference the value obtained by the standard ISO 10456 (corresponding to the most exhaustive and laborious calculation), the SBTC provides design U-values that are consistently lower than the façade real values, with errors between -2.27% in Madrid and -2.77% (Seville) for average annual conditions (Table 6). Thus, it would be necessary to reduce the U-value of these façades to ensure actual compliance with the design requirements under the actual operating conditions of these cities. In addition, the different U-values of the façade configurations in Valencia and Seville are not identified by the SBTC.

Table 6. Design U-values of façade configurations using different approaches (standard ISO 10456; current SBTC; original CCF value; and proposed adjustment C_A) and its comparative errors.

The correction using $CCF_{original}$ values minimises these errors in a functional way, determining the design U-value with greater accuracy by considering the environmental conditions of each location. In general, although the

correction is significant in all cases (the error ranges between +0.65% and +0.92%), some variability remains between façade locations and typologies. This uncertainty is reduced by applying the new factor C_A; the errors regarding standard ISO 10456 decrease to 0.22% in Madrid (10 times lower than the SBTC error and 3 times lower than the correction by $CCF_{original}$). In Valencia and Seville, the improvement is equally effective, and none of the errors exceed 0.23%. This enhanced precision is evident, even having used the average C_A value of the façade subgroup instead of the C_A factor corresponding to each specific façade configuration.

These results demonstrate the usefulness of both the characterisation of the CCF values throughout southern Spain and their subsequent optimisation through the new factor C_A. This improved method constitutes valuable progress towards more precise and reliable performance-based building codes, simultaneously minimising the necessary calculation effort. In the future, the same analysis should be extended to the northwest of the country, until a complete characterisation of the Spanish territory is achieved. The improved correction could also be implemented in other countries in the same way, simply considering the maximum U-values associated with each climatic zone and usual façade configurations (i.e., thus tabulating the applicable C_A values for each of them).

However, it must be remembered that this correction does not consider other environmental effects such as rain, wind or solar radiation on façade materials. Although the analysed regions present low rainfall (a low exposure to wind-driven rain is foreseeable), the high solar radiation typical of the entire Mediterranean Basin can increase the temperature of the façade materials and the necessary corrections. Likewise, the effects of fluctuations in temperature and relative humidity in a lower temporal range (days or hours) have not been considered, which can lead to exceptional corrections significantly higher than those identified based on monthly data. Neither the possible variation of these corrections in scenarios of climate change or the possible use of innovative materials in the façade configurations have been analysed. Quantifying these effects remains a future challenge to refine this functional correction.

5. Conclusions

Using a recent calculation procedure, the necessary corrections have been determined so that the design λ-values of façade materials can be approximated to the real values under the operating conditions of southern Spain. Consulting climatic data that are usually available and incorporating an adjustment factor that considers the specific

façade configuration and the climatic zone of the location, it has been possible to obtain improved design λ-values in a simplified way (by a simple multiplication) with a precision comparable to those calculated by the standard ISO 10456. These findings open the door to using material thermal properties adjusted to the environmental conditions of each place, which will result in improved thermal designs of building façades within the framework of performance-based building codes. This improved correction methodology can also be extrapolated to any other national building code that establishes constant values of thermal conductivity for materials and that defines thermal design requirements based on climatic zones (regardless of the range of climatic conditions).

In turn, the isopleth map and the proposed C_A factors (Fig. 3 and Table 5) allow a functional incorporation of these corrections to the Spanish Building Technical Code, without substantially increasing the current calculation effort. The results confirm the need to correct the standardised λ_{Ib}-values currently used in Spain for building materials. In any point of the analysed territory and for any month of the year, these standardised λ_{Ib}-values are lower than those actually existing under operational conditions, assuming an optimistic insulating performance for the thermal designs of façades. This results in an underlying error, which can lead to inadequate designs and energy consumptions greater than initially expected. The largest corrections have been identified on the coast of the country (especially in the southeast, with average annual corrections above +4% and summer maximums of up to +6% over standardised λ_{Ib}-values).

Acknowledgements

This research was partially funded by the Foundation for the Promotion of Applied Scientific Research and Technology in Asturias (FICYT) through the GRUPIN project Ref. IDI/2018/000221, and The Spanish Ministry of Science, Innovation and Universities through the State Plan for Scientific and Technical Research and Innovation with the project Ref. PGC2018-098459-B-I00, both co-financed with EU FEDER funds. We also recognise engineers D. Lázaro Herrero, J. Sangoluisa Galba and R.Q. Serrat Albano for their assistance with data collection and processing.

References

[1] M. dell'Isola, F.R. d'Ambrosio, G. Giovinco, E. Ianniello, Experimental analysis of thermal conductivity for building materials depending on moisture content, Int. J. Thermophys. 33 (2012) 1674-1685. https://doi.org/10.1007/s10765-012-1215-z

[2] Y. Liu, C. Ma, D. Wang, Y. Wang, J. Liu, 2016. Nonlinear effect of moisture content on effective thermal conductivity of building materials with different pore size distributions, Int. J. Thermophys. 37:56. https://doi.org/10.1007/s10765-016-2062-0

[3] Y.Y. Wang, C. Ma, Y.F. Liu, D.J. Wang, J.P. Liu, Effect of moisture migration and phase change on effective thermal conductivity of porous building materials, Int. J. Heat Mass. Tran. 125 (2018) 330-342. http://dx.doi.org/10.1016/j.ijheatmasstransfer.2018.04.062

[4] F. Ochs, W. Heidemann, H. Müller-Steinhagen, Effective thermal conductivity of moistened insulation materials as a function of temperature, Int. J. Heat. Mass. Tran. 54 (2008) 539-752. https://doi.org/10.1016/j.ijheatmasstransfer.2007.05.005

[5] U. Berardi, M. Naldi, The impact of the temperature dependent thermal conductivity of insulating materials on the effective building envelope performance, Energ. Buildings. 144 (2017) 262-275. https://doi.org/ 10.1016/j.enbuild.2017.03.052

[6] I. Asadi, P. Shafigh, Z.F.B. Abu Hassan, N.B. Mahyuddin, Thermal conductivity of concrete – A review, J. Build. Eng. 20 (2018) 81-93. https://doi.org/10.1016/j.jobe.2018.07.002

[7] M. Abuku, H. Janssen, J. Poesen, S. Roels, Impact, absorption and evaporation of raindrops on building facades, Build. Environ. 44:1 (2009) 113-124. https://doi.org/10.1016/j.buildenv.2008.02.001

[8] M. O'Grady, A.A. Lechowska, A.M. Harte, Quantification of heat losses through building envelope thermal bridges influenced by wind velocity using the outdoor infrared thermography technique, Appl. Energ. 208 (2017) 1038-1052. https://dx.doi.org/10.1016/j.apenergy.2017.09.047

[9] P. Redweik, C. Catita, M. Brito, Solar energy potential on roofs and facades in an urban landscape, Sol. Energy. 97 (2013) 332-341. https://dx.doi.org/10.1016/j.solener.2013.08.036

[10] H.M. Künzel, Effect of interior and exterior insulation on the hygrothermal behaviour of exposed walls, Mater. Struct. 31:2 (1998) 99-103. https://doi.org/10.1007/BF02486471

[11] J.A. Clarke, P.P. Yaneske, A rational approach to the harmonization of the thermal properties of building materials, Build. Environ. 44 (2009) 2046-2055. https://doi.org/10.1016/j.buildenv.2009.02.008

[12] F.G.N. Li, A.Z.P. Smith, P. Biddulph, I.G. Hamilton, R. Lowe, A. Mavrogianni, E. Oikonomou, R. Raslan, S. Stamp, A. Stone, A.J. Summerfield, D. Veitch, V. Gori, T. Oreszczyn, Solid-wall U-values: heat flux measurements compared with standard assumptions, Build. Res. Inf. 43:2 (2015) 238-252. https://doi.org/10.1080/09613218.2014.967977

[13] N.C. Bajali, M. Mani, B.V. Venkatarama, Dynamic thermal performance of conventional and alternative building wall envelopes, J. Build. Eng. 21 (2019) 373-395. https://doi.org/10.1016/j.jobe.2018.11.002

[14] CIBSE Guide A: Environmental design 2015, Thermal properties of building structures. Chartered Institution of Building Services Engineers London, Norwich, 2015.

[15] ISO 12524 Building materials and products – Hygrothermal properties – Tabulated design values, European Committee for Standardization (2000) Brussels, 2000.

[16] DIN 4108-4 Thermal insulation and energy economy in buildings - Part 4: Hygrothermal design values, German Institute for Standardization, Berlin, 2017.

[17] Spanish Ministry of Public Works and Transport, Catálogo informático de elementos constructivos [*Computer catalogue of construction elements*]. https://itec.cat/cec/, 2018 (accessed 4 November 2019).

[18] ISO 10456 Building materials and products - Hygrothermal properties - Tabulated design values and procedures for determining declared and design thermal values, International Organization for Standadization, Geneva, 2007.

[19] ASHRAE Handbook of Fundamentals, Heat, air and moisture control in building assemblies, American Society of Heating, Refrigerating and Air Conditioning Engineers, Atlanta, 2017.

[20] The Building Regulations, Approved Document L1.A - Conservation of fuel and power in new dwellings, Section 4, British Ministry of Housing, Communities and Local Government, London, 2010.

[21] Código Técnico de la Edificación, Documento Básico HE-1 Limitación de la demanda energética *[Spanish Building Technical Code, Basic Document HE 1 Limitation of energy demand]*, Spanish Ministry of Housing, Madrid, 2006.

[22] F. Domínguez, B. Anderson, J.M. Cejudo, A. Carrillo, Uncertainty in the thermal conductivity of insulation materials. Energ. Buildings, 42 (2010) 2159–2168. https://doi.org/10.1016/j.enbuild.2010.07.006

[23] A. Prada, F. Cappelletti, P. Baggio, A. Gasparella, On the effect of material uncertainties in envelope heat transfer simulations, Energ. Buildings. 71 (2014) 53-60. https://dx.doi.org/10.1016/j.enbuild.2013.11.083

[24] C. van Deonkelaar, M. Dowson, E. Burman, C. Spataru, D. Mumovic, 2016. A review of the energy performance gap and its underlying causes.in non-domestic buildings, Front. Mech. Eng. 1:17. https://doi.org/10.3389/fmech.2015.00017

[25] W. Belazi, S.-E. Ouldboukhitine, A. Chateauneuf, A. Bouchair, Uncertainty analysis of occupant behavior and building envelope materials in office building performance simulation, J. Build. Eng. 19 (2018) 434-448. https://doi.org/10.1016/j.jobe.2018.06.005

[26] A. Prada, G. Pernigotto, P. Baggio, A. Gasparella, Uncertainty propagation of material properties in energy simulation of existing residential buildings: The role of buildings features, Build. Simul. 11:3 (2018) 449-464. https://doi.org/10.1007/s12273-017-0418-4

[27] Fraunhofer IBP, Software WUFI. https://wufi.de/en/, 2018 (accessed 4 November 2019).

[28] J.M. Pérez, J. Domínguez, E. Cano, J.J. del Coz, F.P. Álvarez, A correction factor to approximate the design thermal conductivity of building materials: Application to Spanish façades, Energ. Buildings. 88 (2015) 153-164. https://dx.doi.org/10.1016/j.enbuild.2014.12.005

[29] J.M. Pérez, J. Domínguez, E. Cano, M. Alonso, J.J. del Coz, Detailed territorial estimation of design thermal conductivity for façade materials in North-Eastern Spain, Energ. Buildings. 102 (2015) 266-276. https://dx.doi.org/10.1016/j.enbuild.2015.05.025

[30] A. Ioannou, L.C.M. Itard, Energy performance and comfort in residential buildings: Sensitivity for building parameters and occupancy, Energ. Buildings. 92:1 (2015) 216-233. https://doi.org/10.1016/j.enbuild.2015.01.055

[31] U. Berardi, L. Tronchin, M. Manfren, B. Nastasi, 2018. On the Effects of Variation of Thermal Conductivity in Buildings in the Italian Construction Sector, Energies. 11, 872. https://doi.org/10.3390/en11040872

[32] J. Jeon, J. Lee, Y. Ham, Quantifying the impact of building envelope condition on energy use, Build. Res. Inf. 47:4 (2019) 404-420. https://doi.org/10.1080/09613218.2018.1448959

[33] M. Krus, Moisture transport and storage coefficients of porous mineral building materials - Theoretical principles and new test methods. Fraunhofer IRBVerlag, Stuttgart, 1996.

[34] B. Seng, C. Magniont, S. Lorente, Characterization of a precast hemp concrete block. Part II: Hygric properties, J. Build. Eng. 24 (2019) 100579. https://doi.org/10.1016/j.jobe.2018.09.007

[35] P.E. Glaser, I.A. Black, R.S. Lindstrom, F.E. Ruccia, A.E. Wechsler, Thermal insulation systems - A survey. NASA Report SP5027, Washington, 1967.

[36] J.E. Martabid, C. Mourgues, 2015. Criteria used for selecting envelope wall systems in Chilean residential projects. J. Constr. Eng. M. ASCE. 141, 12. https://doi.org/10.1061/(ASCE)CO.1943-7862.0001025.

[37] National Building Code of Finland, Document C4 Thermal insulation guidelines, Section 4, Finnish Ministry of the Environment, Helsinki, 2003.

[38] Irish Building Regulations, Technical Guidance Document L – Conservation of fuel and energy – Dwellings, Section 0.3, Irish Department of Housing, Planning and Local Government, Dublin, 2017.

[39] M. Krus, A. Holm, Simple methods to approximate the liquid transport coefficients describing the absorption and drying process, Proceedings V Symposium Building Physics in the Nordic Countries 241-248. Goteborg, 1999.

[40] Código Técnico de la Edificación, Documento de Apoyo DA DB-HE/2 - Comprobación de limitación de condensaciones superficiales e instersticiales en los cerramientos *[Spanish Building Technical Code, Associated document DA DB-HE/2 - Verifying of the limitation of surface and interstitial condensation in enclosures]*, Spanish Ministry of Housing, Madrid, 2006.

[41] Directive 2010/31/EU of the European Parliament and of the Council of 19 May 2010 on the energy performance of buildings (recast), European Parliament; Official Journal of the European Union L 153, Strasbourg, 2010.

[42] M.C. Peel, B.L. Finlayson, T.A. Mcmahon, Updated world map of the Köppen-Geiger climate classification. Hydrol. Earth. Syst. Sci. 11 (2007) 1633-1644. https://doi.org/10.5194/hess-11-1633-2007

[43] Iberian Climate Atlas: Air, temperature and precipitation 1971-2000, Page 18. State Meteorological Agency of Spain, Madrid, 2011.

[44] Agrarian Information System of Murcia, Custom agrometeorological report. http://siam.imida.es/apex/f?p=101:46:4155785947173661, 2019 (accessed 4 November 2019).

[45] Institute of Agricultural Research and Training of the Junta of Andalucía, Agroclimatic stations. https://www.juntadeandalucia.es/agriculturaypesca/ifapa/ria/servlet/FrontController?action=Init, 2019 (accessed 4 November 2019).

[46] Spanish Ministry of Agriculture, Fisheries, Food and Environment, Agroclimatic information system for irrigable lands. http://eportal.mapama.gob.es/websiar/SeleccionParametrosMap.aspx?dst=1, 2019 (accessed 4 November 2019).

[47] Valencian Association of Meteorology Josep Peinado, Statistics of the meteorological network. https://www.avamet.org/mx-temperatura-mitjana.php, 2019 (accessed 4 November 2019).

[48] Valencian Institute of Agricultural Research, Data of weather stations. http://riegos.ivia.es/, 2019 (accessed 4 November 2019).

[49] Spanish Ministry of Public Works and Transport, Catálogo de Elementos Constructivos – version impresa previa [*Catalogue of construction elements – previous printed version*]. https://www.codigotecnico.org/images/stories/pdf/aplicaciones/nCatalog_infoEConstr/CAT-EC-v06.3_marzo_10.pdf, 2010 (accessed 4 November 2019).

[50] B. Rodríguez, J. Domínguez, J.M. Pérez, J.J. del Coz, Review of international regulations governing the thermal insulation requirements of residential buildings and the harmonization of envelope energy loss, Renew. Sustain. Energy Rev. 34 (2014) 78-90. http://dx.doi.org/10.1016/j.rser.2014.03.009

[51] M. Carpio, J. Jódar, M.L. Rodríguez, M. Zamorano, A proposed method based on approximation and interpolation for determining climatic zones and its effect on energy demand and CO_2 emissions from buildings, Energ. Buildings. 87 (2015) 253-264. https://doi.org/10.1016/j.enbuild.2014.11.041

[52] K. Verichev, M. Carpio, Climatic zoning for building construction in a temperate climate of Chile, Sustain. Cities. Soc. 40 (2018) 352-364. https://doi.org/10.1016/j.scs.2018.04.020

Table 1. The four reference conditions (Ia, Ib, IIa, IIb) established by standard ISO 10456 for declared thermal values.

Reference condition (*)	**Ia**	**Ib**	**IIa**	**IIb**
Temperature	10 ºC	10 ºC	23 ºC	23 ºC
Moisture content	ψ_{dry}	$\psi_{23ºC,50\%\ relative\ humidity}$	ψ_{dry}	$\psi_{23ºC,50\%\ relative\ humidity}$

(*) These conditions also incorporate the ageing effect of the material throughout its useful life.

Table 2. Distribution of weather stations throughout the 6 analysed regions (25 stations were also analysed in neighbouring regions).

Region	Area (km^2)	Population (million)	Inhabitants per km^2	Analysed stations	Distribution (results/km^2)	Distribution (results/inhab.)
Andalusia	87,268	8.370	96.38	97	1 / 900	1 / 86,292
Castile-La Mancha	79,463	2.031	25.96	40	1 / 1,987	1 / 50,787
Community of Madrid	8,022	6.377	806.00	7	1 / 1,146	1 / 911,052
Extremadura	41,635	1.079	25.92	33	1 / 1,262	1 / 32,704
Region of Murcia	11,313	1.463	129.34	63	1 / 180	1 / 44,341
Valencian Community	23,255	4.935	213.30	76	1 / 306	1 / 64,934
	250,956	**25.256**	**100.64**	**316**	**1 / 794**	**1 / 79,926**

Table 3. Mean annual CCF values identified in southern Spain (maximum and minimum monthly values are also shown). *For succinctness, only the most extreme values are presented.*

Region	Location	Latitude (DD)	Longitude (DD)	Altitude (m)	(*) Years analysed	Mean *CCF* (%)	Maximum *CCF* (%)		Minimum *CCF* (%)	
Region of Murcia	San Javier	37.7910	-0.8198	7	2000/15	+4.16	+6.01	Aug	+2.76	Jan
Valencian Community	Sueca	39.2129	-0.3132	1	2008/15	+4.15	+6.03	Aug	+2.77	Jan
Region of Murcia	Murcia (La Vereda)	37.8975	-1.2684	140	2000/15	+4.15	+5.91	Aug	+2.77	Jan
Valencian Community	Sumacàrcer	39.0946	-0.6312	70	2010/15	+4.14	+5.97	Aug	+2.73	Jan
Valencian Community	Teulada	38.7405	0.0965	205	2006/15	+4.11	+5.95	Aug	+2.66	Jan
Region of Murcia	Mazarrón	37.5615	-1.4011	94	2000/15	+4.04	+5.74	Aug	+2.79	Jan
Valencian Community	Gandia	38.9660	-0.1824	22	2006/15	+4.04	+5.81	Aug	+2.72	Jan
Valencian Community	Pego	38.8482	-0.1360	81	2011/15	+4.02	+5.82	Jul	+2.55	Jan
Region of Murcia	Aguilas (La Pilica)	37.4181	-1.5922	31	2000/15	+4.01	+5.68	Aug	+2.76	Jan
Region of Murcia	Aguilas	37.4181	-1.5922	65	2000/15	+4.01	+5.68	Aug	+2.76	Jan
Region of Murcia	Torre Pacheco (Infiernos)	37.8232	-0.9317	92	2000/15	+4.00	+5.73	Aug	+2.69	Jan
Valencian Community	Pilar de la Horadada	37.8680	-0.8126	77	2000/15	+3.99	+5.72	Aug	+2.71	Jan
Andalusia	Almería	36.8348	-2.4025	21	2001/15	+3.99	+5.58	Aug	+2.83	Jan
Valencian Community	Tavernes de Valldigna	39.0946	-0.2382	15	2000/15	+3.98	+5.77	Aug	+2.68	Jan
Valencian Community	Almoradi	38.0308	-0.7747	74	2000/15	+3.98	+5.74	Aug	+2.66	Jan
Valencian Community	Crevillente	38.2402	-0.7833	94	2000/15	+3.96	+5.68	Aug	+2.63	Jan
Valencian Community	Catral	38.1525	-0.8057	27	2000/15	+3.95	+5.72	Aug	+2.55	Jan
Region of Murcia	Roche	37.6275	-0.9193	130	2000/15	+3.94	+5.64	Aug	+2.67	Jan
Region of Murcia	Murcia (La Alberca)	37.9394	-1.1348	56	2001/15	+3.93	+5.66	Aug	+2.55	Jan
Andalusia	Adra	36.7462	-2.9923	14	2001/15	+3.93	+5.42	Aug	+2.81	Jan
Valencian Community	Alicante	38.3694	-0.5000	85	2006/15	+3.93	+5.69	Aug	+2.46	Jan
Andalusia	Puerto de Santa María	36.6045	-6.1645	9	2011/15	+3.92	+5.15	Aug	+2.70	Feb
Andalusia	Isla Mayor	37.1130	-6.1212	35	2005/15	+3.92	+5.16	Jul	+2.84	Jan
Andalusia	Chipiona	36.7503	-6.3998	7	2001/15	+3.91	+5.17	Aug	+2.83	Jan
Valencian Community	Mutxamel	38.4411	-0.4701	63	2006/15	+3.90	+5.56	Aug	+2.52	Jan
…	…	…	…	…	…	…	…		…	
Castile–La Mancha	Marchamalo	40.6801	-3.2098	692	2007/16	+2.91	+4.25	Jul	+1.85	Feb
Valencian Community	Morella	40.6237	-0.1002	1010	2001/15	+2.83	+4.41	Aug	+1.62	Jan
Andalusia	Puebla de D. Fadrique	37.8755	-2.3818	1110	2001/15	+2.81	+4.18	Aug	+1.68	Jan
Castile–La Mancha	Armuña de Tajuña	40.5297	-3.0139	759	2007/16	+2.80	+4.12	Jul	+1.75	Dic
Castile–La Mancha	Jadraque	40.9265	-2.9466	808	2007/16	+2.79	+4.21	Jul	+1.74	Dic
Castile–La Mancha	Villaconejos de Trabaque	40.4129	-2.3248	810	2007/16	+2.71	+4.14	Jul	+1.60	Dic
Andalusia	Jerez del Marquesado	37.1899	-3.1499	1212	2001/15	+2.69	+4.01	Aug	+1.60	Jan
Castile–La Mancha	Mariana	40.1518	-2.1415	940	2007/16	+2.60	+3.97	Aug	+1.52	Dic
Castile–La Mancha	Cañete	40.0278	-1.6501	1053	2007/16	+2.59	+4.08	Aug	+1.49	Jan
Castile–La Mancha	Prados Redondos	40.7954	-1.7986	1129	2007/16	+2.43	+3.80	Jul	+1.42	Jan

(*) Both years inclusive.

Table 4. Mean $R_{contribution}$ value required for each subgroup of façade systems according to the thermal transmittance guideline established by the SBTC for each climatic zone.

CCE subgroup of façade system		Climatic zoning for winter (guideline U-value W/m²K)					
		α (0.94)	A (0.50)	B (0.38)	C (0.29)	D (0.27)	E (0.25)
1	Outer masonry layer, without chamber or with non-ventilated air chamber, and inner insulation (17 configurations)	0.451	0.708	0.778	0.831	0.842	0.854
2	Outer masonry layer, ventilated air chamber and inner insulation (7 configurations)	0.629	0.803	0.850	0.886	0.894	0.901
3	Outer masonry layer with continuous coating, without chamber or with non-ventilated air chamber, and inner insulation (60 configurations)	0.346	0.594	0.691	0.765	0.781	0.797
4	Outer insulation layer with continuous coating, without chamber or with non-ventilated air chamber, and inner masonry (14 configurations)	0.432	0.698	0.770	0.825	0.837	0.849
5	Outer masonry layer with continuous coating, ventilated air chamber and inner insulation (11 configurations)	0.539	0.755	0.814	0.858	0.868	0.878
6	Outer masonry layer with discontinuous coating , without chamber or with non-ventilated air chamber, and inner insulation (60 configurations)	0.349	0.602	0.698	0.769	0.785	0.801
7	Outer masonry layer with discontinuous coating , ventilated air chamber, and inner insulation (31 configurations)	0.417	0.669	0.748	0.808	0.821	0.834
8	Outer insulation layer with discontinuous coating, ventilated air chamber, and inner masonry (10 configurations)	0.383	0.672	0.751	0.810	0.823	0.836
9	Masonry layer without insulation (3 configurations)	0.000	0.000	0.000	0.000	0.000	0.000
10	Lightweight façade with ventilated air chamber (5 configurations)	0.594	0.784	0.836	0.875	0.883	0.892
11	Sandwich panel, without chamber or with non-ventilated air chamber (9 configurations)	0.560	0.766	0.822	0.864	0.874	0.883
12	Prefabricated concrete panel, without chamber or with non-ventilated air chamber (10 configurations)	0.577	0.775	0.829	0.870	0.879	0.888
13	Outer reinforced concrete layer, without chamber or with non-ventilated air chamber (20 configurations)	0.579	0.776	0.830	0.870	0.879	0.888
14	Glass fiber reinforced concrete panel, without chamber or with non-ventilated air chamber (10 configurations)	0.572	0.773	0.827	0.868	0.877	0.886
15	Structural timber frame layer with ventilated air chamber (6 configurations)	0.236	0.753	0.894	0.929	0.954	0.980

Table 5. Proposed factor C_A to adjust the original CCF values identified in Spain, considering façade configuration and climatic zone.

CCE subgroup of façade system			Climatic zoning for winter				
		α	A	B	C	D	E
1	Outer masonry layer, without chamber or with non-ventilated air chamber, and inner insulation	1.088	0.867	0.796	0.740	0.728	0.715
2	Outer masonry layer, ventilated air chamber and inner insulation	0.943	0.770	0.720	0.681	0.673	0.664
3	Outer masonry layer with continuous coating, without chamber or with non-ventilated air chamber, and inner insulation	1.152	0.975	0.884	0.810	0.793	0.776
4	Outer insulation layer with continuous coating, without chamber or with non-ventilated air chamber, and inner masonry	1.101	0.877	0.804	0.747	0.734	0.721
5	Outer masonry layer with continuous coating, ventilated air chamber and inner insulation	1.021	0.820	0.758	0.711	0.701	0.690
6	Outer masonry layer with discontinuous coating, without chamber or with non-ventilated air chamber, and inner insulation	1.150	0.967	0.877	0.805	0.788	0.772
7	Outer masonry layer with discontinuous coating, ventilated air chamber, and inner insulation	1.111	0.906	0.827	0.765	0.751	0.736
8	Outer insulation layer with discontinuous coating, ventilated air chamber, and inner masonry	1.132	0.903	0.824	0.763	0.749	0.735
9	Masonry layer without insulation	1.197	1.197	1.197	1.197	1.197	1.197
10	Lightweight façade with ventilated air chamber	0.975	0.790	0.735	0.693	0.684	0.674
11	Sandwich panel, without chamber or with non-ventilated air chamber	1.004	0.808	0.749	0.704	0.694	0.684
12	Prefabricated concrete panel, without chamber or with non-ventilated air chamber	0.990	0.799	0.742	0.699	0.689	0.679
13	Outer reinforced concrete layer, without chamber or with non-ventilated air chamber	0.988	0.798	0.741	0.698	0.689	0.679
14	Glass fiber reinforced concrete panel, without chamber or with non-ventilated air chamber	0.994	0.802	0.744	0.700	0.691	0.681
15	Structural timber frame layer with ventilated air chamber	1.197	0.822	0.673	0.634	0.606	0.578

Table 6. Design U-value of façade configurations using different approaches (standard ISO 10456; current SBTC; original CCF value; proposed adjustment C_A) and its comparative errors.

		Design U-value (m^2K/W) calculated by means of…			
Location	**Façade subgroup**	ISO 10456	SBTC	$CCF_{original}$ value	$CCF_{original}^{C_A}$ value
Madrid	No. 1	0.2730	0.2668 (-2.27%)	0.2748 (+0.66%)	0.2724 (-0.22%)
Valencia	No. 4	0.3897	0.3798 (-2.54%)	0.3933 (+0.92%)	0.3906 (+0.23%)
	No. 12	0.3828	0.3725 (-2.69%)	0.3858 (+0.78%)	0.3823 (-0.13%)
Seville	No. 4	0.3901	0.3798 (-2.64%)	0.3931 (+0.77%)	0.3905 (+0.10%)
	No. 12	0.3831	0.3725 (-2.77%)	0.3856 (+0.65%)	0.3822 (-0.23%)

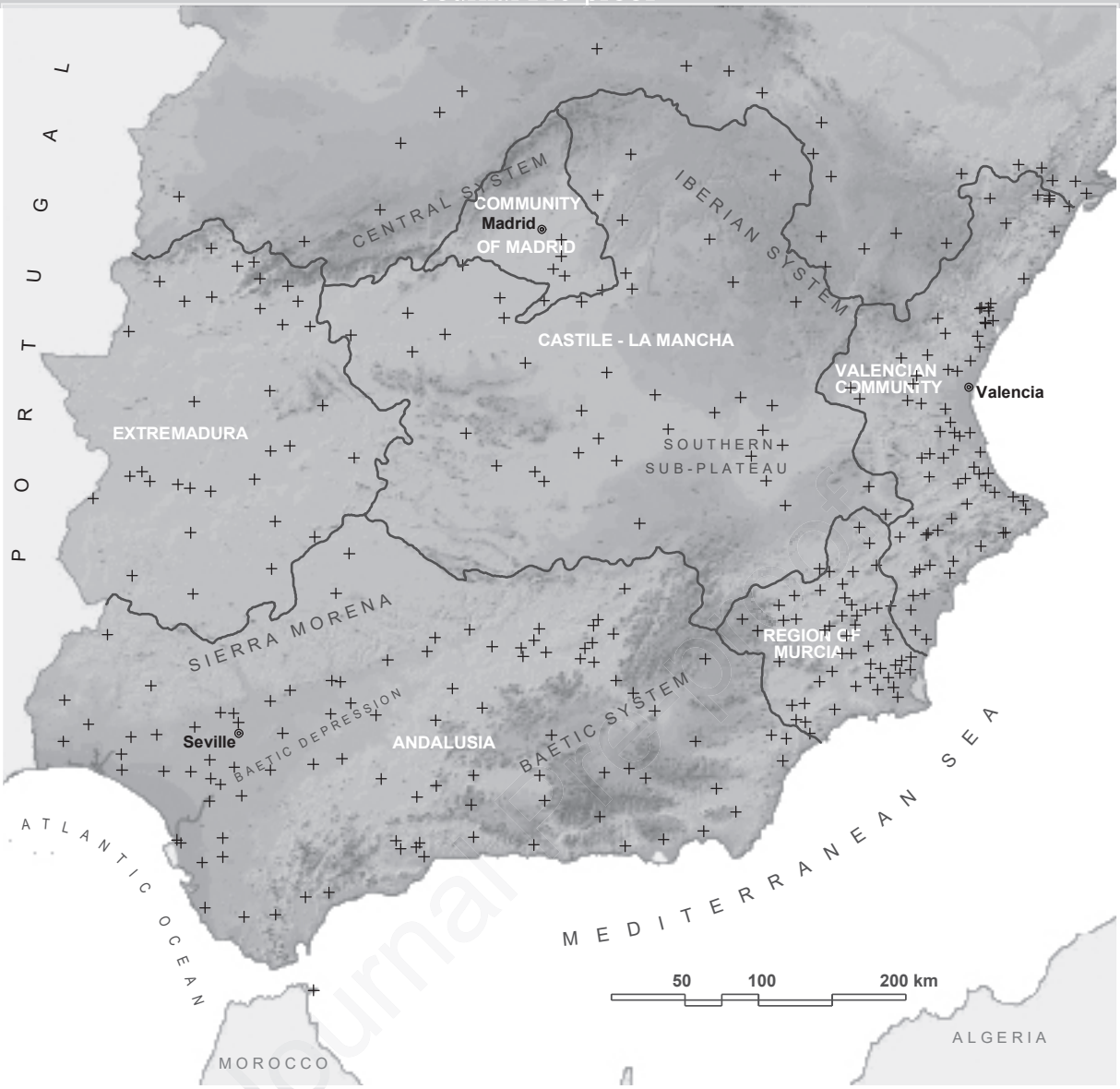

Fig. 2. Territorial distribution of the Spanish weather stations analysed throughout this research. *Darker colours represent higher altitudes*.

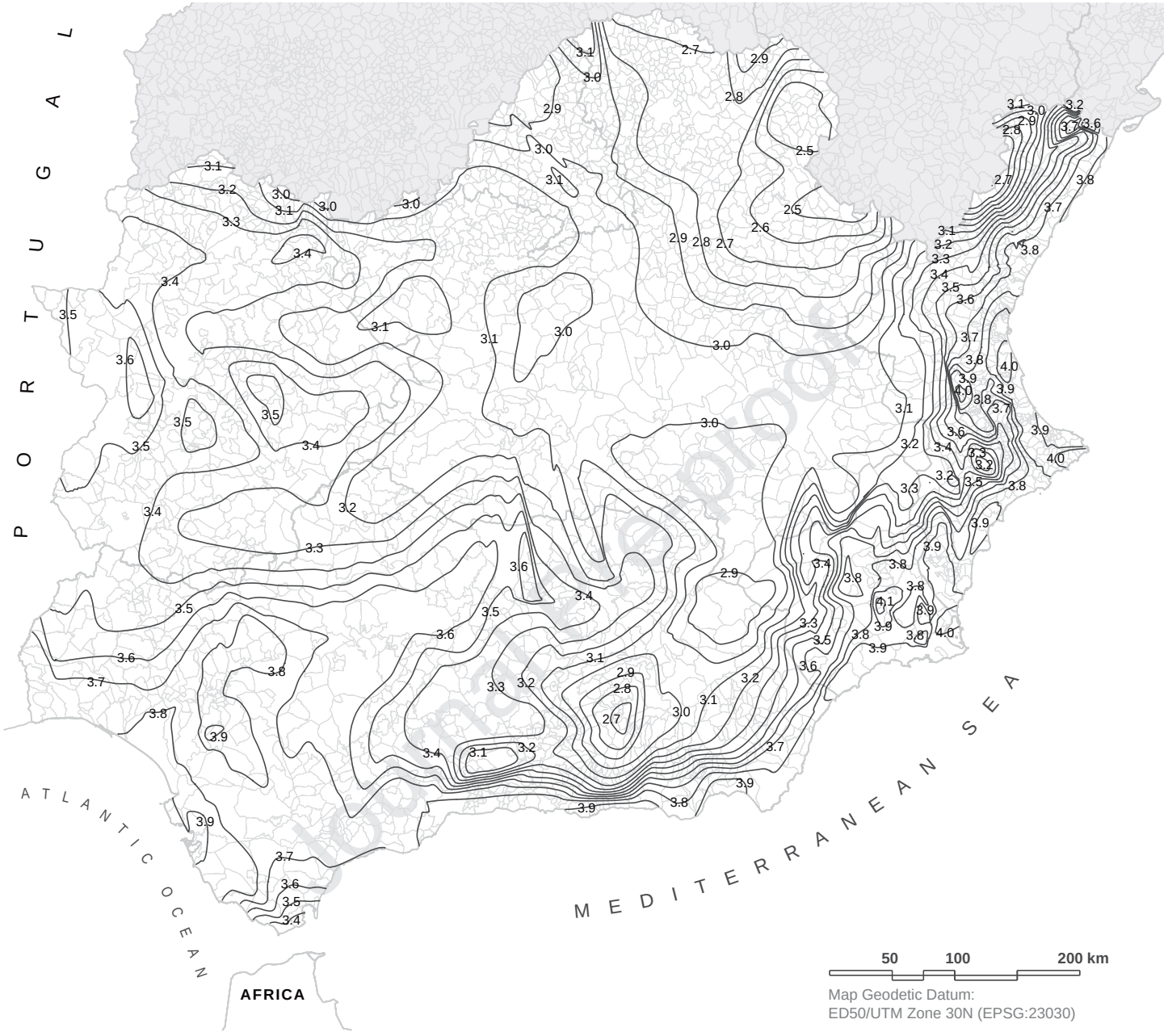

Fig 3. Isopleth map of the mean annual CCF (% values) applicable for façade materials in southern Spain.

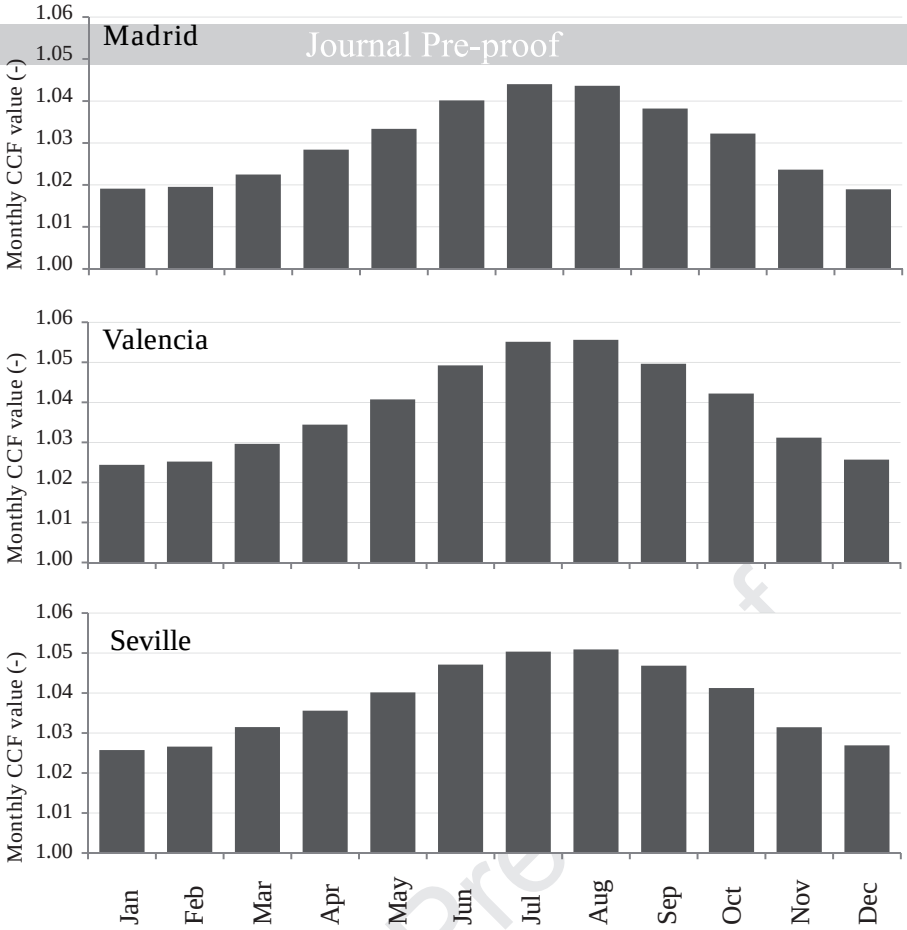

Location		St. Fernando de Henares (Madrid)	Moncada (Valencia)	La Rinconada (Seville)
Latitude (DD)		40.4113	39.5871	37.4562
Longitude (DD)		-03.4966	-00.3991	-05.9247
Altitude (m)		604	35	37
Years analysed		10 (2007/16)	16 (2000/15)	15 (2001/15)
Mean annual T (ºC)		14.03	16.96	17.76
Mean annual RH (%)		62.56	69.36	65.91
Climatic zone		D	B	B
Monthly $CCF_{original}$ values (%)	January	+1.913	+2.442	+2.577
	February	+1.955	+2.522	+2.662
	March	+2.249	+2.966	+3.148
	April	+2.841	+3.442	+3.561
	May	+3.335	+4.073	+4.017
	June	+4.013	+4.923	+4.712
	July	+4.400	+5.515	+5.036
	August	+4.361	+5.561	+5.092
	September	+3.821	+4.965	+4.685
	October	+3.226	+4.219	+4.125
	November	+2.365	+3.120	+3.146
	December	+1.895	+2.572	+2.692
	Mean annual	+3.019	+3.812	+3.770

Fig 4. Annual variation of the monthly $CCF_{original}$ values identified in the largest cities analysed (Madrid, Valencia and Seville) and their mean annual values of temperature and relative humidity.

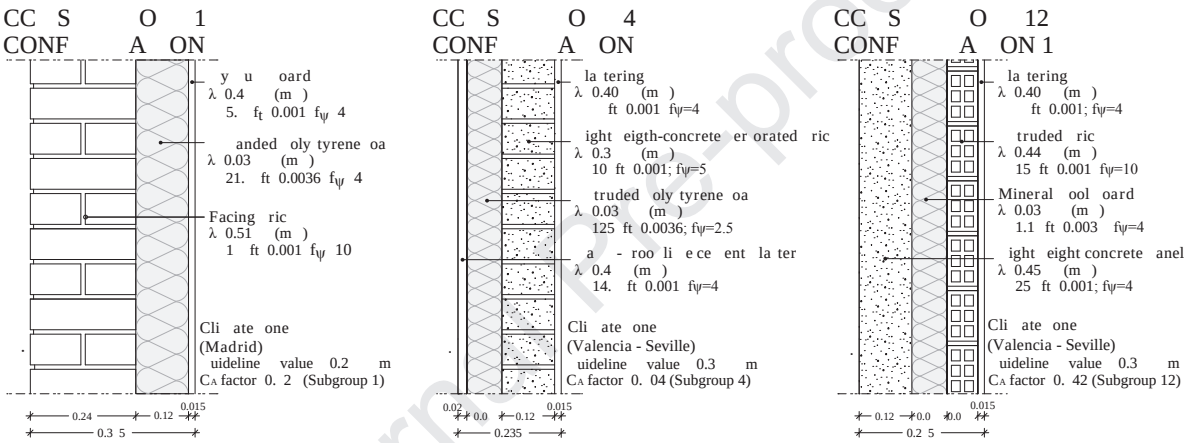

Fig . Fa ade configurations and material properties considered for the validation.

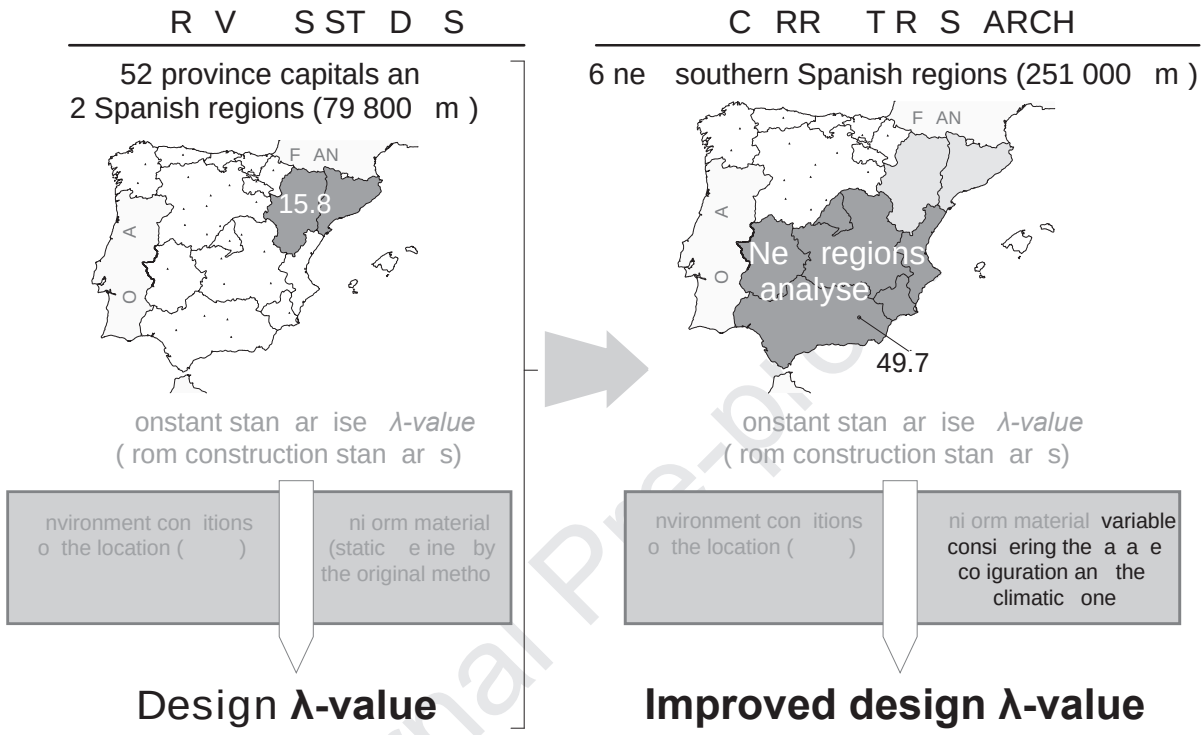

Fig . tension of the application scope and improvements proposed for the calculation procedure.

Highlights

- Calculation procedure to functionally correct the design λ-values of façade materials
- Climate data analysis of 316 locations in 6 regions of southern Spain
- Isopleth map to characterise the applicable corrections in 250.000 km^2 of Spain
- Calculation improvements considering the façade configuration and climatic zoning
- Validation of the improved corrections, regarding the standard ISO 10456 results